ELSEVIER

Journal of Chromatography A, 864 (1999) 271–281

JOURNAL OF CHROMATOGRAPHY A

www.elsevier.com/locate/chroma

Chiral high-performance liquid chromatography of *N*-octyl bicycloheptene dicarboximide and confirmatory studies using liquid chromatography–tandem mass spectrometry and two-dimensional nuclear magnetic resonance spectroscopy

I. Hsiung Wang*, Venkatraman Subramanian, Richard Moorman, Jim Burleson, Jinren Ko

Wellmark International, Inc., 12200 Denton Drive, Dallas, TX 75234, USA

Received 27 April 1999; received in revised form 10 September 1999; accepted 27 September 1999

Abstract

N-Octyl bicycloheptene dicarboximide (MGK 264) has *exo* and *endo* diastereomers. Each structure has a chiral center at the nitrogen side chain. Enantioselective separation of MGK 264 was achieved by normal-phase high-performance liquid chromatography (HPLC) using cellulose-based Chiralcel OD column with diode-array and optical rotation detectors. Peaks were isolated with the purpose of identifying their stereochemical structures. Molecular mass of the HPLC peaks and their structural information was determined by liquid chromatography–electrospray tandem mass spectrometry (LC–ES-MS–MS). A two-dimensional nuclear magnetic resonance (NMR) spectroscopic technique was used to establish the structural features. Correlation of the data obtained from chiral separation and NMR facilitated in unambiguous assignment of the HPLC peaks.

Keywords: Enantiomer separation; *N*-Octyl bicycloheptene dicarboximide

1. Introduction

N-Octyl bicycloheptene dicarboximide (MGK 264) is widely used as a synergist in pyrethrum and certain pyrethroids based insecticide formulation [1–3]. It is well known that different stereochemical isomers or enantiomers of pesticides give entirely different efficacy results. The stereochemical structures of MGK 264, shown in Fig. 1, have *exo* and *endo* structures and each structure contains a chiral center at the nitrogen side chain. Several papers have been reported on the analysis of technical MGK 264 using gas chromatography with flame ionization detection [4]. But there is little mention in the literature on high-performance liquid chromatography (HPLC) analysis for MGK 264, enantiomeric determination or stereochemical structure identification. Recently, we reported reversed-phase HPLC methodologies for the analysis of active ingredients in pesticide formulations [5–7]. Using ternary mobile phase systems and temperature control techniques, the separation of active ingredients in complex formulations could be achieved with high precision. The HPLC method becomes more powerful as an analytical technique when coupled with mass spectrometry (MS) [8–11], which can provide valuable information on structural characteristics and impurities identification.

*Corresponding author.

0021-9673/99/$ – see front matter
PII: S0021-9673(99)01044-4

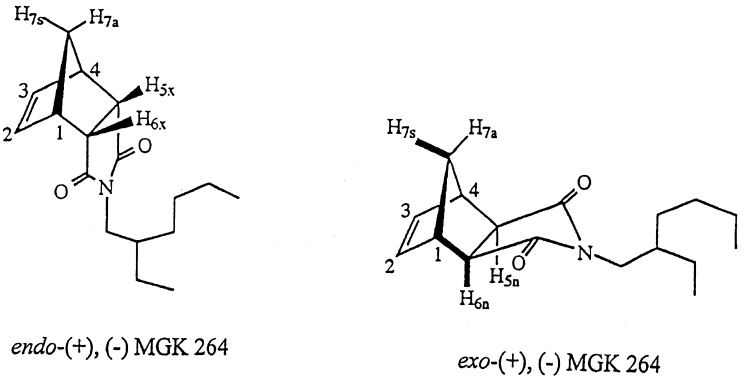

endo-(+), (-) MGK 264

exo-(+), (-) MGK 264

Fig. 1. Stereochemical structures of *exo*- and *endo*-MGK 264.

Chiral columns, the only columns that can separate racemic mixtures, are gaining popularity with the advent of newer and more stable stationary phases [12–15]. Lisseter and Hambling reported the separation and resolution of a large range of synthetic pyrethroid insecticides using Pirkle columns [16]. In this study, we used a chiral stationary phase, which is based on cellulose, a polysaccharide. Using a cellulose-based chiral column with UV detection, the *exo* and *endo* stereoisomers of MGK 264 and their racemic mixtures were separated. The optical rotation of the racemic mixtures was determined by using an optical rotation detector. HPLC peaks identification and their structural features were studied and confirmed by using liquid chromatography–electrospray tandem mass spectrometry (LC–ES-MS–MS) and ^{1}H–^{1}H COSY (correlated spectroscopy) nuclear magnetic resonance (NMR) techniques.

2. Experimental

2.1. Chemicals and materials

Technical grade MGK 264 was obtained from McLaughlin Gormley King (Minneapolis, MN, USA). MGK 264 standard was obtained from Standards and Special Chemistry Group, Wellmark International (Dallas, TX, USA). HPLC grade hexane and isopropanol were purchased from Fisher Scientific (Fairlawn, NJ, USA). The chiral column used was a Chiralcel OD column, obtained from Chiral Technologies (Exton, PA, USA).

2.2. Chiral HPLC analysis

Chiral chromatographic analyses of MGK 264 were carried out on a Hewlett-Packard mode 1090 liquid chromatographic system (Wilmington, DE, USA) equipped with UV and Chiralyser optical rotation (J.M. Science, Grand Island, NY, USA) detectors. Separation was accomplished on a Chiralcel OD (Chiral Technologies) column (250×4.6 mm I.D., 10 μm particle size). The mobile phase was hexane containing 1% isopropanol at a flow-rate of 1.2 ml/min. UV detection was at a wavelength of 205 nm. The column temperature was maintained at 40°C.

2.3. Preparation of exo- and endo-MGK264 samples

The *exo*- and *endo*-MGK 264 isomers were analytically separated and collected from the Hewlett-Packard 1090 HPLC system. Approximately 2 mg of the individual isomer was collected. The HPLC eluents were then evaporated to dryness under nitrogen and redissolved in deuterated chloroform for NMR analysis.

2.4. LC–ES-MS–MS analysis

The HPLC system for the LC–ESI-MS–MS was a Hewlett-Packard 1050 HPLC system. The operating

conditions, e.g., mobile phase, flow-rate etc., were the same as mentioned above. Mass spectral fragmentations were obtained using a Finnigan TSQ 7000 triple-quadrupole mass spectrometer (Finnigan, San Jose, CA, USA) equipped with an electrospray ion source (ESI) and a closed collision gas chamber for detecting and quantifying target compounds in the LC column eluent. The MS was operated in the positive ion mode by applying a voltage of 5.0 kV to the capillary. The ESI vaporizer was operated at 400°C with a heated capillary temperature of 210°C. The mass spectrometer was programmed to transmit the protonated molecular ions through the first quadrupole to the octapole. Here the ions underwent collision-induced dissociation (CID), to the third quadrupole, where the product ions were monitored. The rate of scan was 1.0 scan/s. A collision gas (Ar) pressure of 1.5 mTorr was employed and the collision offsets were 10 V, 15 V and 30 V multiple energy (1 Torr=133.322 Pa).

2.5. NMR analysis

^{1}H-NMR spectra of *exo*- and *endo*-MGK 264 were recorded at ambient temperature on a Varian 300 spectrometer operating at 300 MHz and using deuterated chloroform as solvent. The ^{1}H-NMR spectra were collected in 16 480 data points over a 3500.2 Hz spectral width, with a 45° pulse width of 7.0 μs and a relaxation delay of 1 s. Two-dimensional COSY NMR spectra were collected in a 1024× 512 matrix with a spectral width of 2964.7 Hz. The chemical shifts are expressed as δ, ppm.

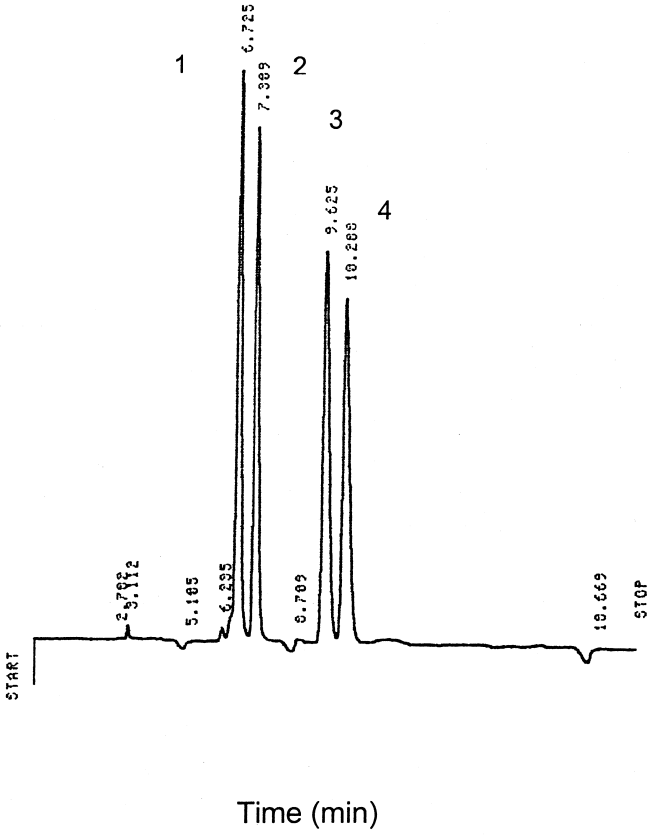

Fig. 2. Chiral separation of MGK 264 on Chiralcel OD column (25×0.46 cm); mobile phase: hexane–isopropanol (99:1); flow-rate: 1.2 ml/min; Oven temperature: 40°C; UV wavelength: 205 nm. Peaks: 1=*exo*-(+)-MGK 264, 2=*exo*-(−)-MGK 264, 3=*endo*-(+)-MGK 264, 4=*endo*-(−)-MGK 264.

3. Results and discussion

3.1. Chiral high-performance liquid chromatographic MGK 264 separation

Fig. 2 shows the complete chiral separation for four enantiomers of MGK 264 which was achieved on a cellulose-based phase Chiralcel OD column with UV detection (205 nm). Retention factors k_1 and k_2 (t_0=3 min for 1,3,5-tributylbenzene) for peaks 1 and 2 were 0.55 and 0.59. For the second pair of peaks, 3 and 4, the retention factors were k_3=0.69 and k_4=0.71. To determine the (+) isomers and (−) isomers and to confirm the enantiomeric pairs, an optical rotation detector was used. Peaks 2 and 4 showed negative peak responses corresponding to (−) isomers. A comparison of the diode array detection for peaks 1 and 2 (*exo*-MGK 264) and peaks 3 and 4 (*endo*-MGK 264) is shown in Fig. 3A and B, respectively. A more pronounced red shift at approximately 210 nm was observed for *endo*-MGK 264 compared to *exo*-MGK 264. This may be explained by a more efficient conjugation of the lone pair of electrons on the nitrogen with the carbonyl groups in the *endo* isomer.

Hydrogen-bonding interaction or dipole–dipole interactions with the carbamate moiety in the stationary phase are considered to be crucial for chiral resolution [17]. It can be postulated that the carboximide moiety of the molecule would be the most likely interaction site with carbamate functionalities of the stationary phase. Since the *endo* isomer has an ''L'' shaped configuration vs. a linear configuration for the *exo* isomer, it could be surmised that the *endo* isomer would have greater interaction with the stationary phase compared the *exo* isomer. This results in the *endo* isomer eluting after the *exo* isomer.

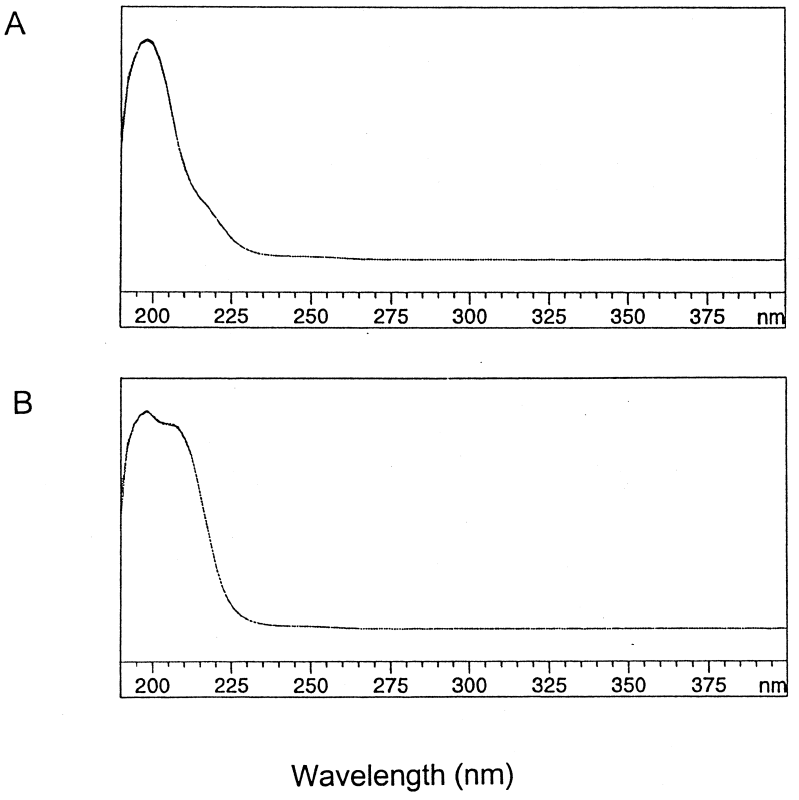

Fig. 3. UV–Vis diode array absorption spectra for *exo*-MGK 264 (top, λ_{max}=198 nm) and *endo*-MGK 264 (bottom, λ_{max}=190 nm) in the mixture of water, acetonitrile and methanol.

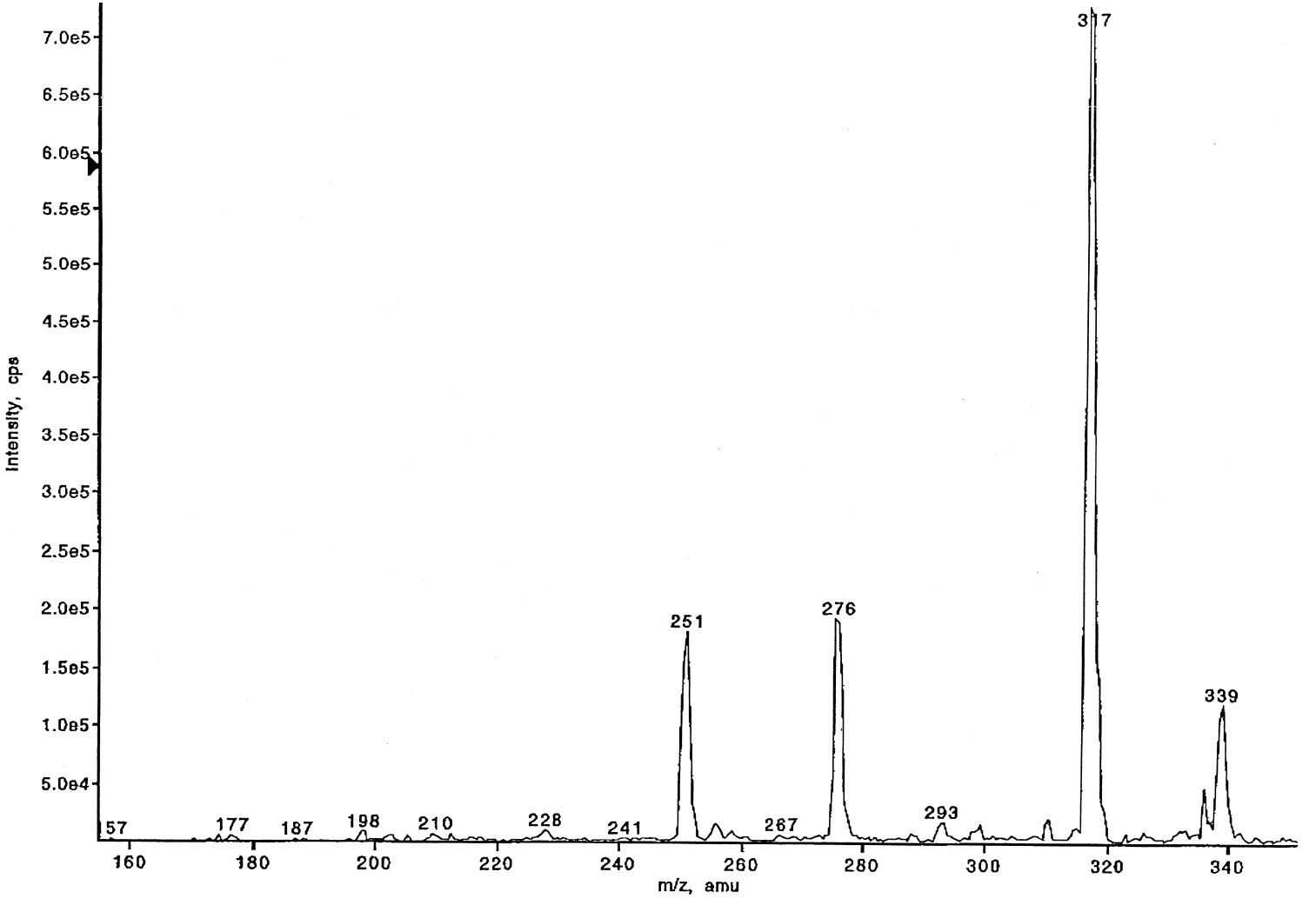

Fig. 4. LC–ES-MS–MS spectrum of *exo*-MGK 264. The dominant ion occurs at m/z 317, corresponding to $[MH+CH_3CN]^+$.

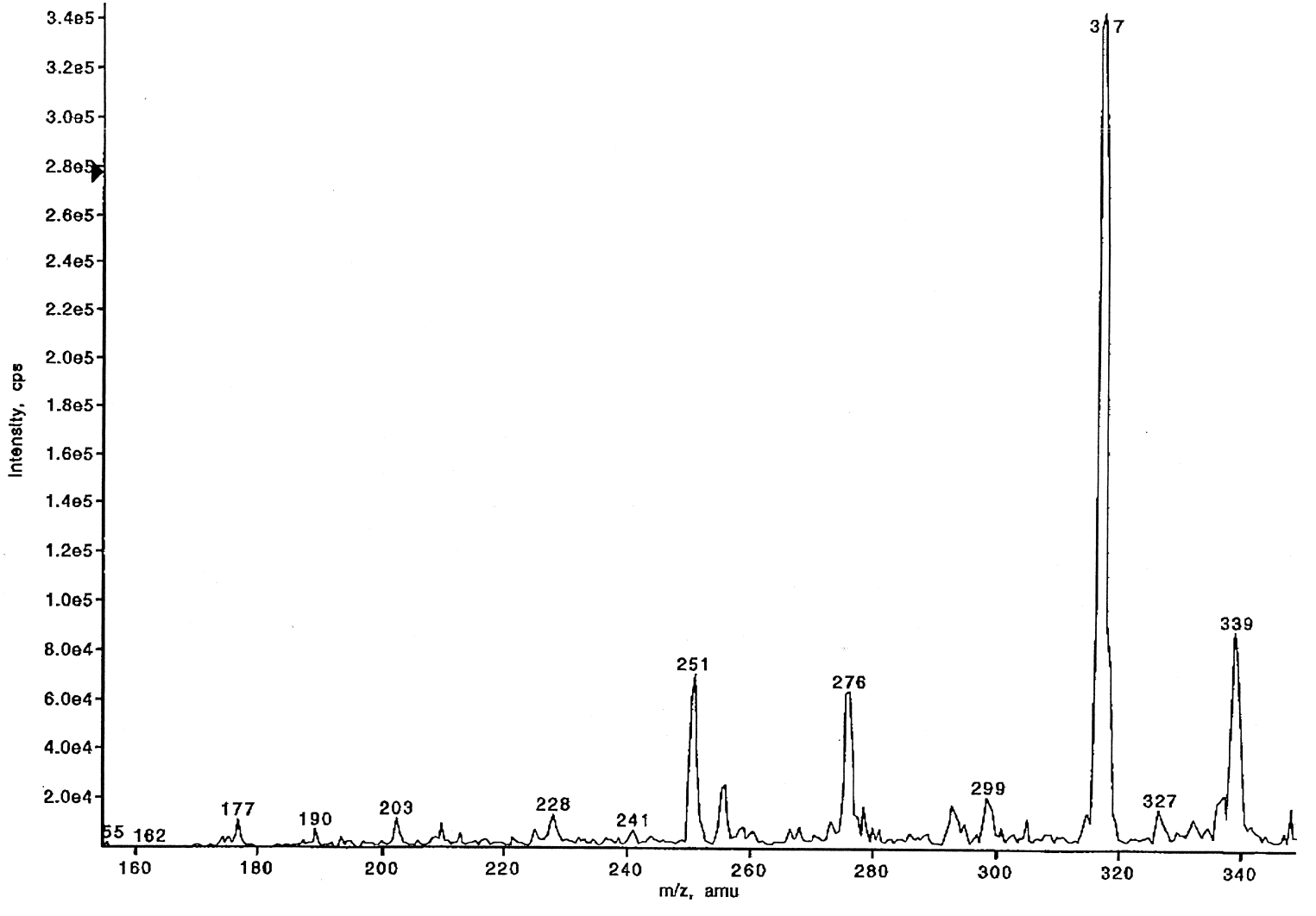

Fig. 5. LC–ES-MS–MS spectrum of *endo*-MGK 264. The dominant ion occurs at m/z 317, corresponding to $[MH+CH_3CN]^+$.

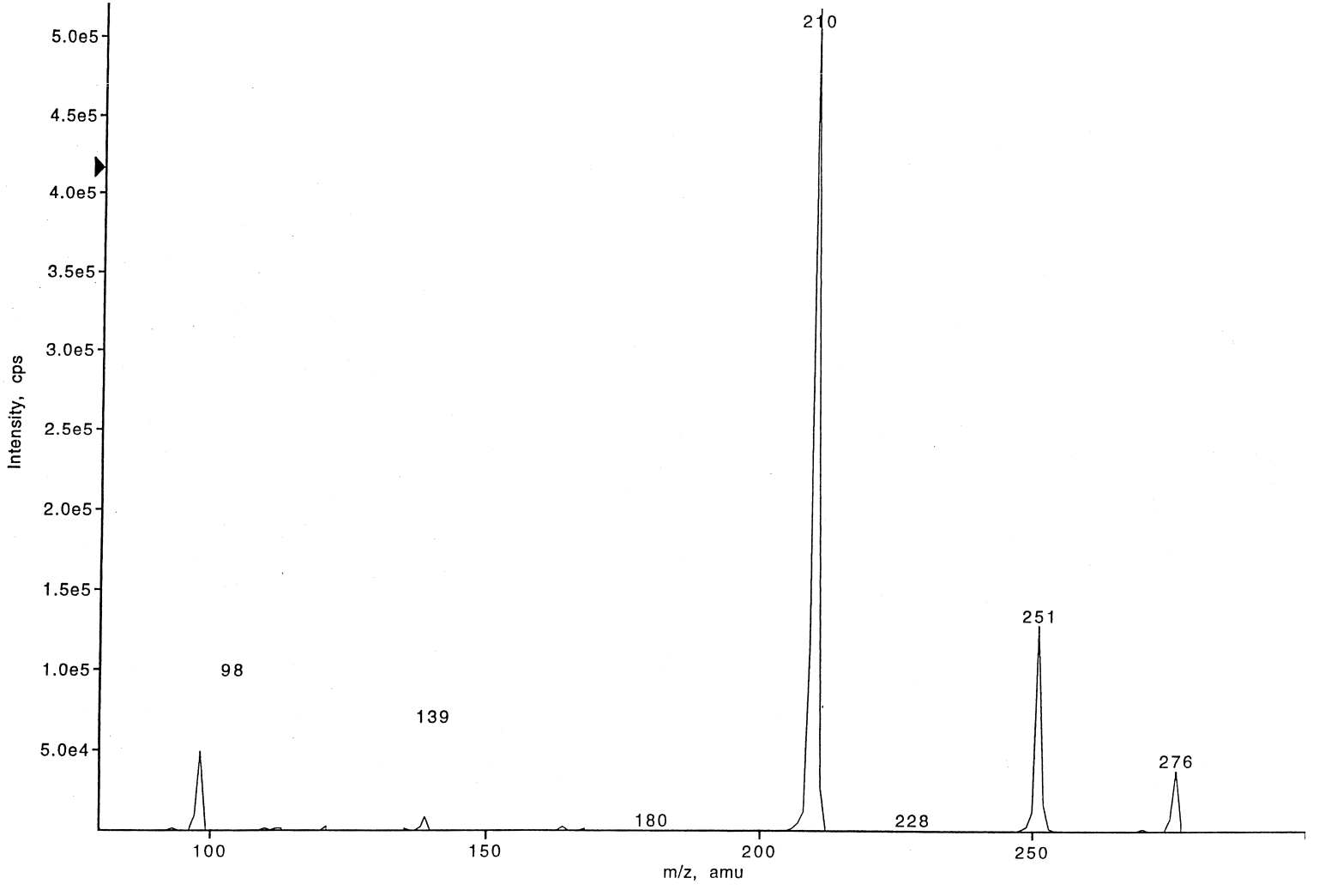

Fig. 6. Product ion spectrum of $[M+H]^+$ at m/z 276. The ion was isolated and then collisionally dissociated producing predominantly retro-Diels–Alder fragment at m/z 210.

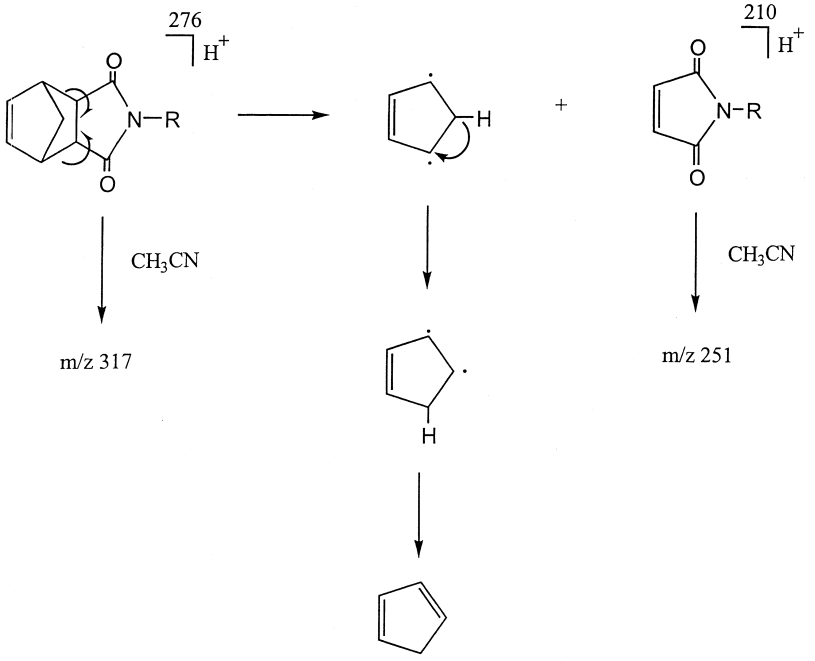

Fig. 7. Schematic representation of the major fragmentation reactions of MGK 264.

3.2. Peak assignment of chiral HPLC MGK 264 analysis

The *exo*- and *endo*-MGK 264 isomers were further characterized by LC–ES-MS–MS. The HPLC eluent peaks were isolated in order to confirm their stereochemical structures by using a two-dimensional ^{1}H–^{1}H COSY NMR technique.

The use of LC–MS was not only to confirm the structural information of MGK-264 but also to detect weak or non-UV-absorbing eluents. The ESI-MS mass spectra of *exo*-MGK264 and *endo*-MGK 264 are shown in Figs. 4 and 5. The ESI-MS mass spectra of *exo*- and *endo*-MGK 264 HPLC peaks had the same spectra with dominant ions at m/z 317, $[MH+CH_3CN]^+$, and other ions at m/z 276, $[M+H]^+$, 251 $[210+CH_3CN]^+$ and 339 $[M+CH_3CN+Na]^+$. The complete structure elucidation of MGK 264 could be obtained by means of tandem mass spectrometry (MS–MS). Monitoring of the selected precursor and product ion pairs using ESI-MS–MS indicated that common fragmentation pathways existed. Isolation of the protonated molecular ion at m/z 276 followed by collisional dissociation pro-

Table 1
^{1}H-NMR data for *exo*-MGK 264

Proton type (No. proton)	Chemical shift δ (ppm) (multiplicity)	Coupling constant J (Hz)
Methyl (6H)	0.85 (t)	7.4
Methylene and H_{7a} (9H)	1.15–1.40 (m)	
H_{7s} (1H)	1.50 (AB)	10.6
NCH_2CH (1H)	1.70 (m)	
H_{5n}, H_{6n} (2H)	2.65 (m)	
H_1, H_4 (2H)	3.25 (m)	
NCH_2 (2H)	3.35 (d)	7.4
H_2, H_3 (2H)	6.27 (m)	

Table 2
^{1}H-NMR data for *endo*-MGK 264

Proton type (No. proton)	Chemical shift δ (ppm) (multiplicity)	Coupling constant J (Hz)
Methyl (6H)	0.85 (t)	7.4
Methylene (8H)	1.15–1.35 (m)	
H_{7s} or H_{7a}(1H)	1.52 (AB)	8.5
NCH_2CH (1H)	1.60 (m)	
H_{7s} or H_{7a} (1H)	1.82 (AB)	8.5
NCH_2 (2H)	3.20 (m)	
H_{5x}, H_{6x} (2H)	3.22 (m)	
H_1, H_4 (2H)	3.37 (m)	
H_2, H_3 (2H)	6.20 (m)	

duced the retro-Diels–Alder rearrangement ion at m/z 210 in high yield, as shown in Fig. 6. The m/z 210 fragment ion could then be used for quantitation. The m/z 98 arose from α cleavage through the adjacent carbon–nitrogen bond and m/z 139 due to the loss of large alkyl group, while the formation of m/z 251 involved the adduction of m/z 210 and CH_3CN. Carefully control the source conditions such as orifice voltage can lead to the reduction of m/z 317 and 339. The m/z 210 is due to the in source fragmentation of MGK 264, then with the adduction of CH_3CN, which leads to the m/z 251 as shown in

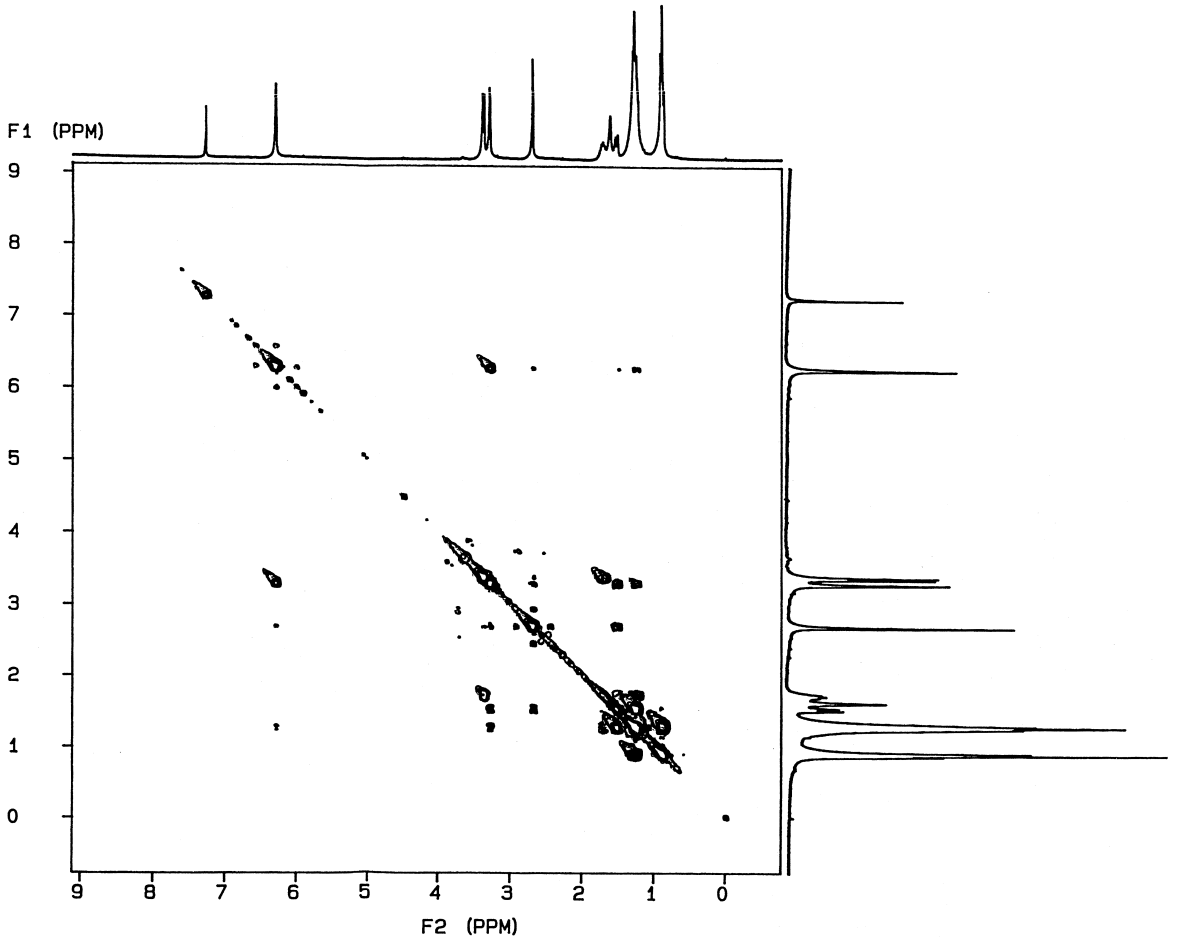

Fig. 8. Contour plot of two-dimensional proton COSY spectrum of *exo*-MGK 264.

Fig. 7. Product ion spectrum of MGK 264 at *m/z* 251 showed the same characteristic fragmentation behavior, e.g., *m/z* 210→*m/z* 251, *m/z* 210→*m/z* 98.

LC–MS provides mass and structural information of the eluent peaks. However, it has limitations for distinguishing between certain isomers and identifying functional groups. In order to elucidate the structural features of the isomers, NMR technique was used in this study. The ^{1}H-decoupled NMR spectra of *exo*-MGK 264 or *endo*-MGK 264 did not show significant signal enhancement by Nuclear Overhauser Effect (NOE). Two-dimensional NMR technique gives information such as connectivity and proximity more efficiently and unambiguously. These results allowed us to distinguish the MGK 264 stereochemical isomers from each other. The peak assignments are shown in Tables 1 and 2. Peak area of the absorptions of the proton nuclei were in agreement with their relative abundances. Protons, H_{5x} and H_{6x} (δ 3.22) in norborene derivatives are deshielded relative to the corresponding isomeric H_{5n} and H_{6n} (δ 2.65). This helped in establish the configuration of these protons in norbornenes bearing substituents in the 5 and 6 ring position. The difference between *exo* and *endo* proton chemical shifts in norbornenes was ascribed to the magnetic anisotropy of the 2,3 double bond in this system [18]. The H_{7s} also displayed four bonds $^{4}J_{HH}$ long-range couplings via ''W'' path in this rigid bicyclohexane system with H_{6n} and H_{5n} [19–21]. The COSY spectra (Figs. 8 and 9) confirmed the

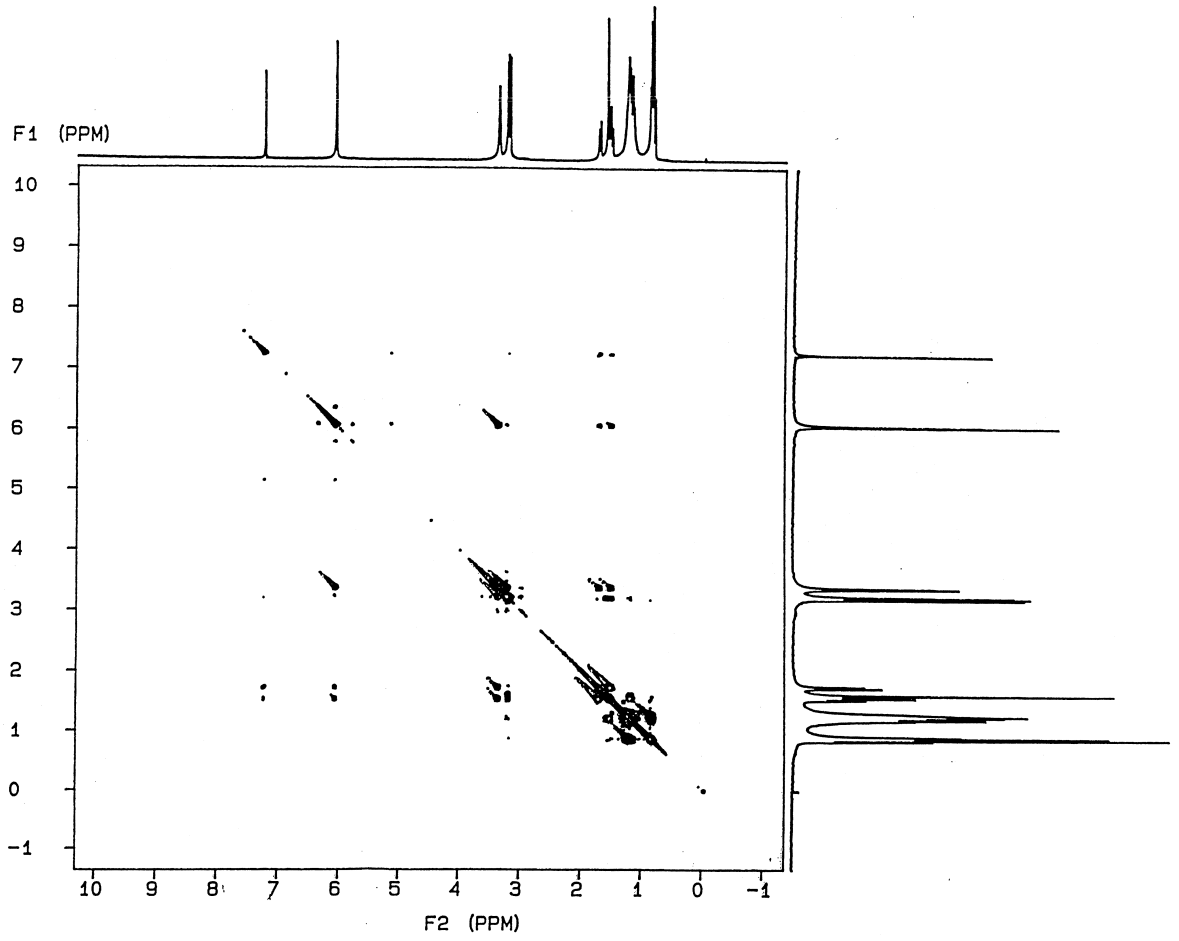

Fig. 9. Contour plot of two-dimensional proton COSY spectrum of *endo*-MGK 264.

connectivity of coupled nuclei described above. The H_{7s} was not only coupled with H_{7a} (J_{AB}=10.6 Hz) but also showed strong $^{4}J_{HH}$ coupling with H_{6n} and H_{5n}. From the above results, we could assign that the first pair of eluent peaks was *exo*-MGK264, and the second pair of eluent peaks was *endo*-MGK 264.

4. Conclusions

Chiral HPLC using cellulose-based columns was shown to completely separate four enantiomers of MGK 264. Optical rotation detector facilitated in assigning the (+) and (−) isomers for *exo* and *endo* MGK264. LC–MS–MS provided information for the structural characterization of *exo*- and *endo*-MGK 264 HPLC eluted peaks. A two-dimensional NMR technique confirmed their stereochemical structural identities such as connectivity and proximity more efficiently and unambiguously. This eventually helped in assigning the first pair of eluting peaks to the *exo*-MGK 264 and the latter pair to the *endo* isomer.

Acknowledgements

The authors gratefully acknowledge Professor Alan P. Marchand of the University of North Texas (Denton, TX, USA) for the COSY NMR spectra, and Dr. Allan Xu of KeyStone Analytical Labs. (North Wales, PA, USA) for the LC–ES-MS–MS spectra. We also thank JM Science (Grand Island, NY, USA) for providing a Chiralyser optical detector and the McLaughlin Gormley King (Minneapolis, MN, USA) for supplying MGK 264 sample. Finally, the authors wish to thank Wellmark International for permission to publish this work.

References

[1] C.-F. Chang, S. Tamura, Appl. Entomol. Zool. 6 (1971) 143.
[2] C.-F. Chang, S. Murakoshi, S. Tamura, Agric. Biol. Chem. 36 (1972) 692.
[3] S. Murakoshi, C.-F. Chang, S. Tamura, Agric. Biol. Chem. 36 (1972) 695.
[4] K.T. Nguyen, R. Moorman, V. Kuykendall, J. AOAC Int. 18 (1998) 503.
[5] I.-H. Wang, R. Moorman, J. Burleson, J. Liq. Chromatogr. 19 (1996) 3293.
[6] I.-H. Wang, V. Subramanian, R. Moorman, J. Burleson, J. Ko, J. Chromatogr. A 766 (1997) 277.
[7] I.-H. Wang, V. Subramanian, R. Moorman, J. Burleson, J. Ko, D. Johnson, LC·GC 17 (1999) 260.
[8] M.A. Baldwin, F.W. McLafferty, Biomed. Mass Spectrom. 7 (1973) 1111.
[9] W.M.A. Niessen, A.P. Tinke, J. Chromatogr. A 703 (1995) 37.
[10] E. Gelpi, J. Chromatogr. A 703 (1995) 59.
[11] J. Slobodink, B.L.M. van Baar, U.A.Th. Brinkman, J. Chromatogr. A 703 (1995) 81.
[12] Y. Okamoto, M. Kawashima, R. Abreratani, K. Hatada, T. Nishiyama, M. Masuda, Chem. Lett. (1986) 1237.
[13] Y. Okamoto, Y. Kaida, J. Chromatogr. A 666 (1994) 403.
[14] A.M. Krstulovic, J. Pharm. Biomed. Anal. 6 (1988) 641.
[15] H.Y. Aboul-Enein, M.R. Islam, Labmedica 5 (1988) 27.
[16] S.G. Lisseter, S.G. Hambling, J. Chromatogr. 539 (1991) 207.
[17] Y. Okamoto, Y. Kaida, J. High Resolut. Chromatogr. 13 (1990) 708.
[18] J.L. Marshall, S.R. Walter, M. Barfield, A.P. Marchand, N.W. Marchand, A.L. Segre, Tetrahedron 32 (1976) 537.
[19] K.B. Wiberg, D.S. Connor, J. Am. Chem. Soc. 88 (1966) 4437.
[20] M. Barfield, J.L. Marshall, E.D. Canada Jr., M.R. Willcott III, J. Am. Chem. Soc. 100 (1978) 7075.
[21] M. Barfield, J.L. Marshall, E.D. Canada Jr., J. Am. Chem. Soc. 102 (1980) 7.